

Cite this: DOI: 10.1039/c3ra22579h

Synthesis, characterization, and application of a manganese Schiff base complex containing salicylaldehyde–poly(vinylamine)/SBA-15 as a novel heterogeneous hybrid catalyst

Ahmad Reza Massah,^{*ab} Roozbeh Javad Kalbasi^{*ab} and Somayeh Kaviyani^a

A manganese Schiff base complex containing salicylaldehyde–poly(vinylamine)/SBA-15 (Mn–SA–PVAm/SBA-15) composite was prepared as a novel heterogeneous catalyst through *in situ* polymerization of vinylamine within the nano-channels of mesoporous silica SBA-15 without using any organo silica precursors. The catalyst was characterized well by elemental analysis, FT-IR, AAS, DRS UV-Vis, XRD, BET, SEM and TGA techniques. The catalytic activity of the supported metal complex was studied in the selective oxidation of benzyl alcohols using *t*-butyl hydroperoxide as an oxidant. The effects of reaction temperature, solvent and the amount of catalyst as well as the recyclability of the catalyst were investigated.

Received 19th October 2012,

Accepted 2nd May 2013

DOI: 10.1039/c3ra22579h

www.rsc.org/advances

1. Introduction

The oxidation of alcohols to aldehydes and ketones is a widely used chemical transformation in organic synthesis.¹ Transition metal complexes are effective and selective catalysts in the oxidation of alcohols.^{2–4} Schiff base complexes are easy to synthesize and, as well as porphyrins and phthalocyanines, mimic the enzymatic catalysts present in biological systems.^{5,6} The high electron-donating ability of the Schiff base ligand, which facilitates the electron transfer rate, is expected to improve the overall catalytic activity of an imine-functionalized composite.^{7–9} Although transition metal complexes catalysts offer interesting results in organic synthesis, these complexes are still associated with problems of corrosion, contamination of reaction products and difficulties of separation.^{10–12} To overcome these drawbacks, the heterogenization of homogeneous catalysts is expected. Extensive investigations have been focused on the incorporation of metal complex catalysts onto or into inert supports such as molecular sieves, amorphous silica, and polymers.^{13–15} Organic–inorganic hybrid materials are other supports for the heterogenization of homogeneous metal complex catalysts. Organic–inorganic composite materials are increasingly important for a variety of applications due to their extraordinary properties which arise from the combination of the different building blocks. The combination of nanoscale

inorganic moieties with organic polymers has a high potential for future applications.^{16–19} Resultant materials are supposed to have better mechanical and/or thermal properties.²⁰ In these cases the inorganic moiety is a mesoporous molecular sieve crystalline framework material. These porous inorganic solids with empty pores and channels are excellent hosts for intercalation reactions.^{21,22} Silica SBA-15 is a mesoporous molecular sieve, which possesses uniform hexagonal channels ranging from 5 to 30 nm and a very narrow pore-size distribution. Its large internal surface area ($>800 \text{ m}^2 \text{ g}^{-1}$) allows for the dispersion of a large number of catalytically active centers, whereas its thick framework walls (3.1–6.4 nm) provide high hydrothermal stability.^{23–25}

In continuing our previous work to develop new polymer–inorganic hybrid materials as heterogeneous catalysts,^{26–28} herein, we have focused our attention on the synthesis and characterization of a manganese Schiff base complex containing salicylaldehyde–poly(vinylamine) supported on SBA-15 (Scheme 1) as a heterogeneous hybrid catalyst. The catalyst was prepared *via* a simple method without using any organo silica precursors. The catalytic activity of this novel hybrid catalyst was tested for the selective oxidation of alcohols. This catalyst could be reused several times (at least 5) without significant loss of activity/selectivity.

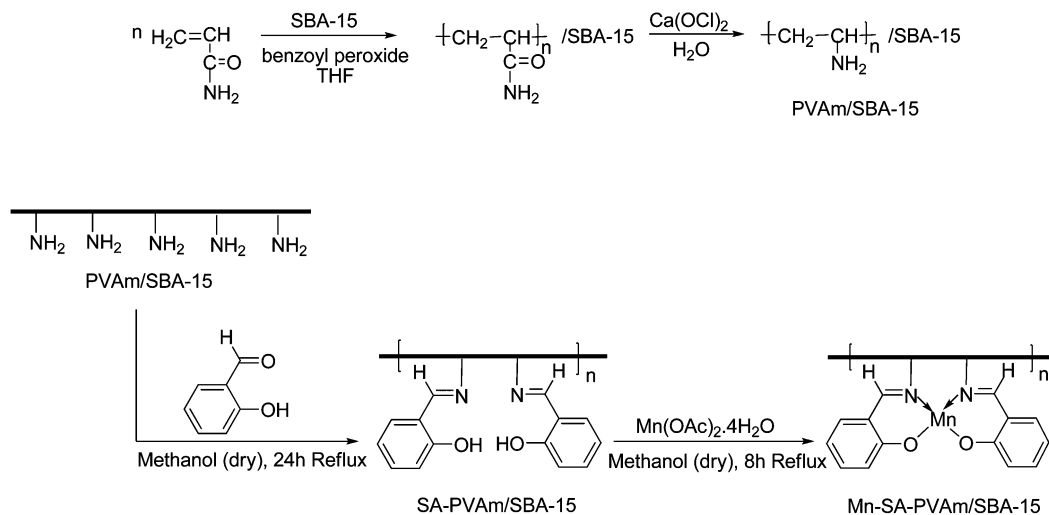
2. Experimental

2.1. Catalyst characterization

The materials were characterized by atomic absorption spectroscopy (AAS) (Perkin-Elmer, Analyst 300), X-ray diffrac-

^aDepartment of Chemistry, Shahreza Branch, Islamic Azad University, 311-86145 Shahreza, Isfahan, Iran. E-mail: massah@iaush.ac.ir; rkalbasi@iaush.ac.ir; Fax: +98-321-3213103; Tel: +98-321-3213211

^bRazi Chemistry Research Center, Shahreza Branch, Islamic Azad University, Shahreza, Isfahan, Iran



Scheme 1 Preparation of Mn-SA-PVAm/SBA-15.

tion (Bruker D8ADVANCE, Cu-K α radiation), FT-IR spectroscopy (Nicolet 400D in KBr matrix in the range 4000–400 cm^{-1}), BET specific surface area and BJH pore size distribution (Series BEL SORP 18, at 77 K), diffuse reflectance (DR) UV-Vis spectroscopy (Shimadzu UV-265), thermo gravimetric analysis (TGA, Setaram Labsys TG (STA) in a temperature range 30–700 $^{\circ}\text{C}$ and with a heating rate of 10 $^{\circ}\text{C min}^{-1}$ in an N_2 atmosphere) and SEM (Philips, XL30, SE detector). The products were identified by ^1H NMR and ^{13}C NMR spectroscopy (Bruker DRX-400 Avance spectrometer at 400 and 100 MHz, respectively). The melting points were measured on an electro-thermal 9100 apparatus and reported without correction. The melting points compared satisfactorily with those reported in the literature.

2.2. Catalyst preparation

2.2.1. Preparation of poly(vinylamine)/SBA-15. Mesoporous silica SBA-15 was prepared through the addition of H_3PO_4 as described in the literature recently.²⁹ The poly(vinylamine)/SBA-15 composite was synthesized as follows:

In the first step, into a 50 mL round-bottomed flask, acrylamide (0.25 g, 3.5 mmol), benzoylperoxide (0.025 g, 0.1 mmol), SBA-15 (1 g) and THF (10 mL) were added. The solution was stirred with a magnetic stirrer and refluxed for 4.5 h at 70 $^{\circ}\text{C}$. Then the solution was filtered and washed with THF (2×5 mL). The white precipitate was dried in air overnight. This composite was named poly(acrylamide)/SBA-15 (PAA/SBA-15). In the second step, into a 100 mL round-bottomed flask PAA/SBA-15 composite (0.5 g), calcium hypochlorite ($\text{Ca}(\text{OCl})_2$) (2 g) and distilled water (75 mL) were added. The solution was stirred with a magnetic stirrer and refluxed for 4.5 h at 90 $^{\circ}\text{C}$. Then the solution was filtered and washed with hot distilled water (2×200 mL). The white precipitate was dried in air overnight. Finally, through the Hoffman reaction, the poly(vinylamine)/SBA-15 (PVAm/SBA-15) composite was obtained.

2.2.2. Preparation of Schiff base ligand containing salicylaldehyde-poly(vinylamine)/SBA-15. Into a 25 mL round-bottomed flask, PVAm/SBA-15 composite (0.5 g), salicylaldehyde

(1.3 mL, 12.4 mmol) and dry methanol (7 mL) were refluxed for 24 h at 70 $^{\circ}\text{C}$ under a nitrogen atmosphere. The yellow precipitate obtained was washed with dry methanol (2×5 mL) to remove excess salicylaldehyde to give a Schiff base ligand containing salicylaldehyde-poly(vinylamine)/SBA-15 (SA-PVAm/SBA-15).

2.2.3. Preparation of manganese Schiff base complex containing salicylaldehyde-poly(vinylamine)/SBA-15. A flask containing a stirred suspension of manganese(II) acetate tetrahydrate (2.45 g, 10 mmol) in 10 mL of dry methanol was purged with nitrogen and then warmed to 40 $^{\circ}\text{C}$ under a nitrogen atmosphere. SA-PVAm/SBA-15 (0.5 g) was added in one portion and the resulting suspension was then refluxed under a nitrogen atmosphere for 8 h at 70 $^{\circ}\text{C}$ to give a manganese Schiff base complex containing salicylaldehyde-poly(vinylamine)/SBA-15 (Mn-SA-PVAm/SBA-15). The collected solid was washed with dry methanol (2×5 mL) and dried in air.

The Mn content of the catalyst was estimated by decomposing a known amount of the catalyst using perchloric acid, nitric acid, fluoric acid, and hydrochloric acid, and the transition metal content was estimated using an atomic absorption spectrometer (Perkin-Elmer, Analyst 300).

2.3. General procedure for the oxidation of alcohols

0.1 g of catalyst and 2 mmol of benzyl alcohol were mixed in 5 mL of CH_3CN and the mixture was refluxed with continuous stirring in an oil bath. 3 mmol of *t*-butyl hydroperoxide (TBHP) was added to the refluxing mixture and the progress of the reaction was monitored by thin layer chromatography (TLC) (eluent: *n*-hexane : ethyl acetate = 16 : 4). After completion of the reaction, the mixture was cooled to room temperature and the catalyst was removed by filtration. Diethyl ether (15 mL) was added to the filtrate and washed with brine (10 mL) and H_2O (10 mL). The organic layer was dried over MgSO_4 and the solvent was evaporated to offer the crude product. The pure product was obtained by column chromatography over silica gel using *n*-hexane/ethyl acetate mixed solvent as the eluent.

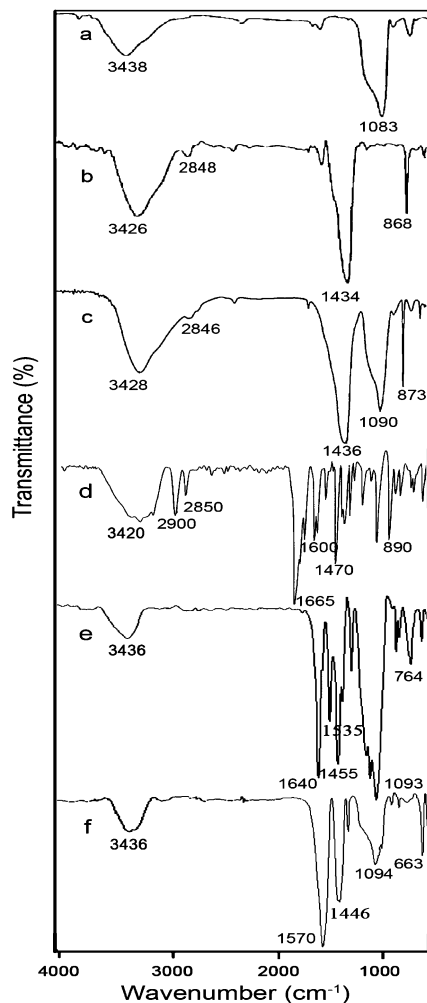


Fig. 1 FT-IR spectra of (a) mesoporous silica SBA-15, (b) PVAm, (c) PVAm/SBA-15, (d) salicylaldehyde, (e) SA-PVAm/SBA-15 and (f) Mn-SA-PVAm/SBA-15.

3. Results and discussion

3.1. Characterization of catalyst

Fig. 1 shows the FT-IR spectra of mesoporous silica SBA-15, PVAm, PVAm/SBA-15, salicylaldehyde, SA-PVAm/SBA-15 and Mn-SA-PVAm/SBA-15. The characteristic band around 1080–1090 cm^{-1} is due to the Si–O stretching in the Si–O–Si structure, which is seen in Fig. 1a, c, e and f. In the FT-IR spectrum of PVAm/SBA-15 (Fig. 1c), the new band at 1436 cm^{-1} is the bending vibration absorption of the N–H bond. Also, the presence of peaks at around 2800–3000 cm^{-1} corresponds to the aliphatic C–H stretching in the PVAm/SBA-15 composite. Moreover, the peak around 3430 cm^{-1} is stronger than in the FT-IR spectrum of SBA-15, which is due to the stretching vibration of the N–H groups. This is in accordance with the spectrum of PVAm (Fig. 1b). In the FT-IR spectra of SA-PVAm/SBA-15 (Fig. 1e) and Mn-SA-PVAm/SBA-15 (Fig. 1f), the peak at around 3430 cm^{-1} is the same as in the FT-IR spectrum of SBA-15 (Fig. 1a), and is due to the stretching vibration of the O–H groups, which shows that amine functional groups are condensed by salicylaldehyde.

Moreover, the presence of peaks at 2800–3000 cm^{-1} corresponds to the aliphatic C–H stretching in SA-PVAm/SBA-15. In addition, in the FT-IR spectrum of SA-PVAm/SBA-15 (Fig. 1e), the sharp band appearing at 1640 cm^{-1} is due to the vibration of C=N. The appearance of the above band shows that salicylaldehyde is attached to the surface of PVAm/SBA-15 and the SA-PVAm/SBA-15 composite is obtained. As shown in the Mn-SA-PVAm/SBA-15 spectrum (Fig. 1f), the band at around 1640 cm^{-1} , which corresponds to C=N, is shifted to lower wave numbers (1570 cm^{-1}) (red shift). This may be due to the interaction between the Mn cations and the C=N groups and the formation of a ligand–metal complex. This means that Mn-SA-PVAm/SBA-15 was successfully prepared.

The powder XRD patterns of the mesoporous silica SBA-15, PVAm/SBA-15, SA-PVAm/SBA-15 and Mn-SA-PVAm/SBA-15 are shown in Fig. 2. The low angle diffraction pattern of SBA-15 shows evidence of three reflections at 2θ values of 0.5–3°, including one strong peak, (100), and two weak peaks, (110) and (200), corresponding to a highly ordered hexagonal mesoporous silica framework.³⁰ The PVAm/SBA-15, SA-PVAm/SBA-15 and Mn-SA-PVAm/SBA-15 samples show the same pattern, indicating that the long-range order of the SBA-15 (100) framework is retained after the hybridization of SBA-15. However, it is observed that the intensity of these characteristic diffraction peaks is decreased in these samples compared with pure mesoporous silica SBA-15, which is probably due to the presence of guest moieties on the mesoporous framework of SBA-15, resulting in a decrease in

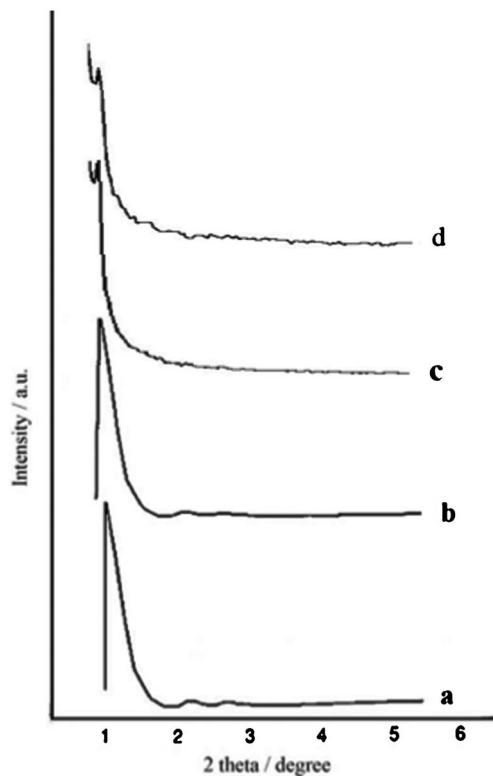


Fig. 2 Powder XRD patterns of (a) mesoporous silica SBA-15, (b) PVAm/SBA-15, (c) SA-PVAm/SBA-15 and (d) Mn-SA-PVAm/SBA-15.

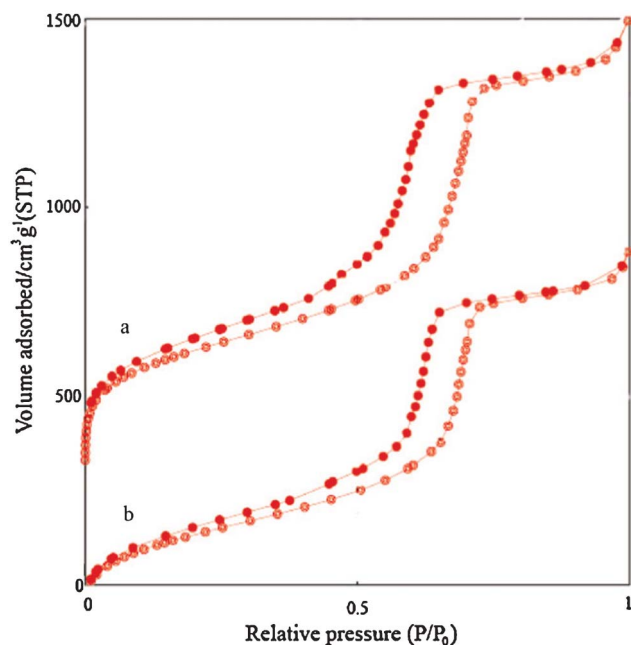


Fig. 3 N₂ adsorption-desorption isotherm of (a) pure SBA-15 and (b) PVAm/SBA-15.

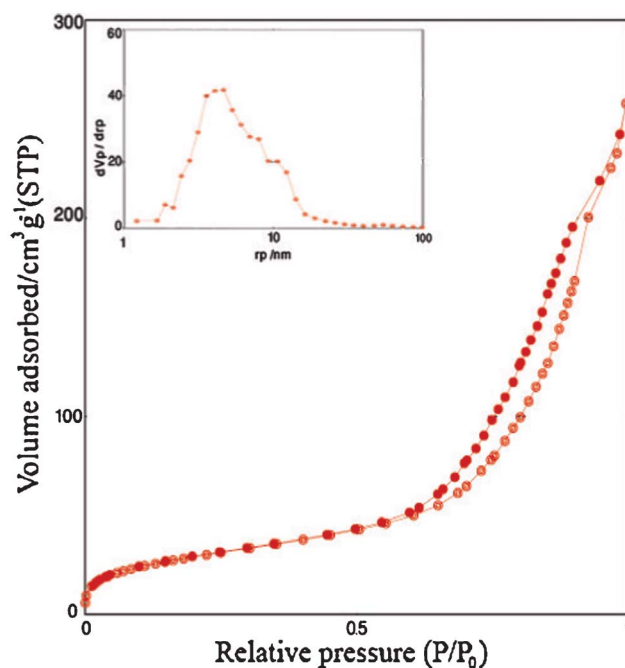


Fig. 4 N₂ adsorption-desorption isotherm and BJH pore size distribution obtained for SA-PVAm/SBA-15.

the crystallinity. In addition, the composites contain much less SBA-15 due to dilution of the silicious material by PVAm, salicylaldehyde and Mn; therefore, this dilution can also account for a decrease in the peak intensity.

The N₂ adsorption-desorption isotherms of the pure SBA-15, PVAm/SBA-15, SA-PVAm/SBA-15 and Mn-SA-PVAm/SBA-15 samples are shown in Fig. 3, 4 and 5. The isotherms are similar to the type IV isotherm with H1-type hysteresis loops at high relative pressure according to the IUPAC classification, characteristic of mesoporous materials with highly uniform size distributions. From the two branches of the adsorption-desorption isotherms, the presence of a sharp adsorption step in the P/P_0 region from 0.6 to 0.8 and a hysteresis loop at the relative pressure $P/P_0 > 0.7$ show that the materials possess a well defined array of regular mesoporous (Fig. 3 and 4). However, there are differences between the Mn-SA-PVAm/SBA-15 sample and the others; the amount of adsorbed nitrogen is lower at the same relative pressure and the step and its sharpness are smaller. This phenomenon implies that the Mn cations are incorporated into the pores of the SBA-15. The specific surface areas and the pore sizes have been calculated using the Brunauer-Emmett-Teller (BET) and Barrett-Joyner-Halenda (BJH) methods, respectively. The structure data of all the mesoporous materials (BET surface area, total pore volume, and pore size) are summarized in Table 1. It is clear that calcined SBA-15 has a high BET surface area ($1430 \text{ m}^2 \text{ g}^{-1}$), and a large pore volume ($1.9 \text{ cm}^3 \text{ g}^{-1}$) and pore size (9.9 nm), indicative of its potential application as a host inorganic material. After hybridization with PVAm through *in situ* polymerization, PVAm/SBA-15 exhibits a smaller specific area, pore size and pore volume in comparison with those of pure SBA-15, which might be due to the presence of polymer on the internal surface of the SBA-15. Although

these textural properties are smaller than those found for mesoporous silica SBA-15, PVAm/SBA-15 still has a mesoporous form and does not block the pores of the SBA-15, hence it is suitable to be developed and grafted with other organic

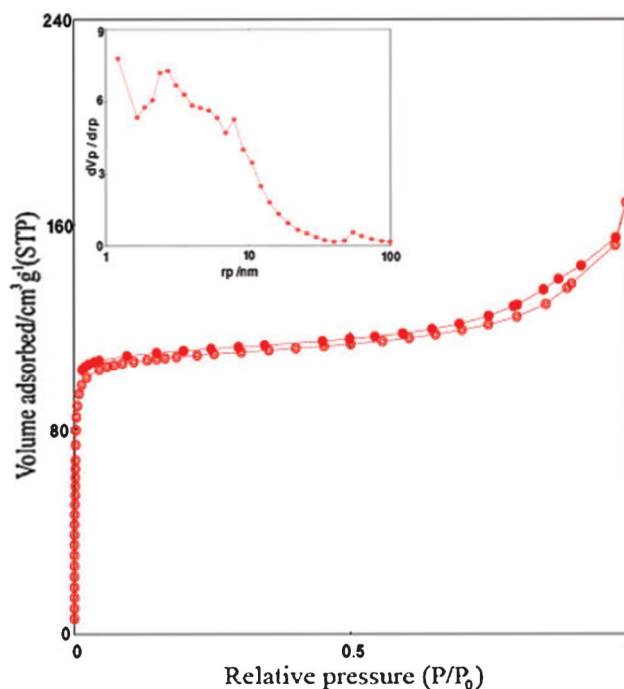
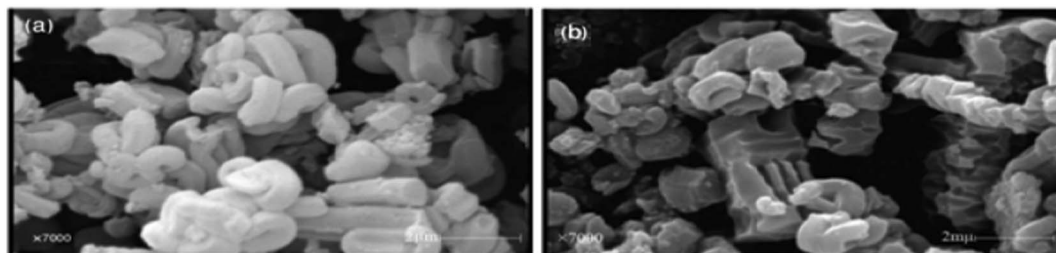


Fig. 5 N₂ adsorption-desorption isotherm and BJH pore size distribution obtained for Mn-SA-PVAm/SBA-15.

Table 1 Surface data of the samples

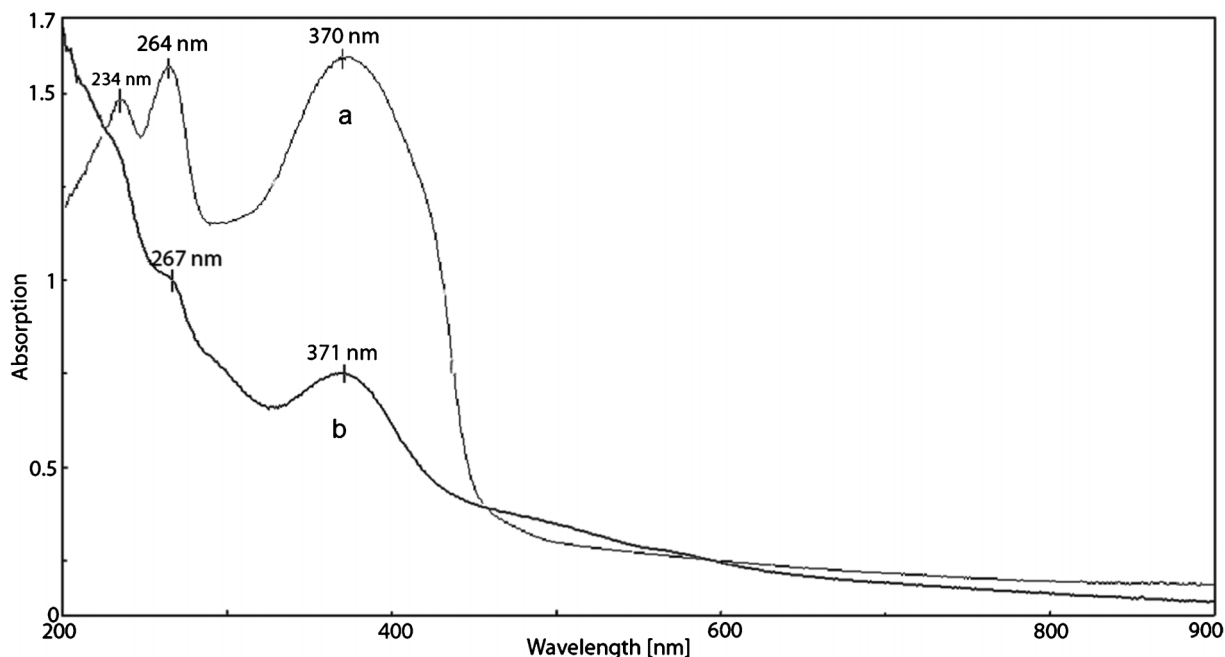
Sample	BET surface area ($\text{m}^2 \text{g}^{-1}$)	Pore volume ($\text{cm}^3 \text{g}^{-1}$)	Pore diameter (nm)
Mesoporous silica SBA-15	1430	1.90	9.90
PVAm/SBA-15	856	1.08	8.81
SA-PVAm/SBA-15	442	0.39	4.89
Mn-SA-PVAm/SBA-15	104	0.25	2.25

**Fig. 6** Scanning electron microscopy (SEM) photographs of (a) SBA-15 and (b) Mn-SA-PVAm/SBA-15.

compounds for the formation of novel ligands. The data for the Mn-SA-PVAm/SBA-15 sample indicates a reduction in surface area, pore size and pore volume compared to SA-PVAm/SBA-15. This might be due to the incorporation of Mn into the channels of SA-PVAm/SBA-15 and the pore size distribution curve for this catalyst proves this idea (Fig. 5, inset). These results are likely to be due to the presence of Mn on the surface of the catalyst. Although these textural properties are smaller than those found for mesoporous silica SBA-15, Mn-SA-PVAm/SBA-15 is still suitable to function as a heterogeneous catalyst.

Fig. 6 shows scanning electron microscopy (SEM) photographs of SBA-15, and the Mn-SA-PVAm/SBA-15 composite. We can see that there is negligible difference in the particle surface morphology between SBA-15 and Mn-SA-PVAm/SBA-15, which indicates that the polymerization, salicylaldehyde grafting and coordination of Mn on the ligand, take place more in the channels and less on the outer surfaces of the catalyst.

The electronic spectral profiles of SA-PVAm/SBA-15 and Mn-SA-PVAm/SBA-15 are reproduced in Fig. 7. The electronic spectrum of the SA-PVAm/SBA-15 exhibits three bands at 370,

**Fig. 7** UV-Vis spectra of (a) SA-PVAm/SBA-15 and (b) Mn-SA-PVAm/SBA-15.

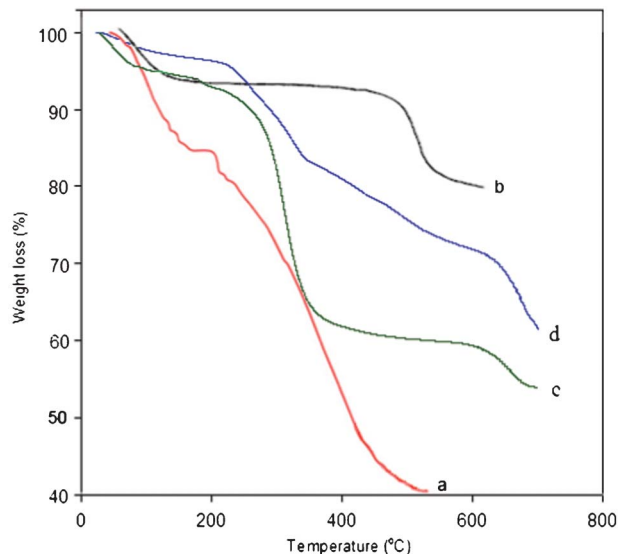


Fig. 8 TGA curves of (a) PVAm, (b) PVAm/SBA-15, (c) SA-PVAm/SBA-15 and (d) Mn-SA-PVAm/SBA-15.

264 and 234 nm and these are assigned to the $n \rightarrow \pi^*$, $\pi \rightarrow \pi^*$ and $\sigma \rightarrow \sigma^*$ transitions, respectively.³¹ These bands shift to higher wavelengths and the intensity of these bands is decreased for Mn-SA-PVAm/SBA-15. However, the $\sigma \rightarrow \sigma^*$ transition is removed indicating the restructuring of the ligand after coordination to the metal ion. The appearance of a weak band due to a ligand to metal transition underneath the $n \rightarrow \pi^*$ transition makes this a band broad. No band could be located in the higher wavelength region due to the expected d-d transition.

Fig. 8 shows the TGA curves of PVAm, PVAm/SBA-15, SA-PVAm/SBA-15 and Mn-SA-PVAm/SBA-15 under an N_2 atmosphere. The weight loss (around 34%, w/w) of PVAm begins at 170 °C because of the thermo-degradation of the PVAm polymer chains and the degradation ends at 550 °C (Fig. 8a); whereas for the PVAm/SBA-15 sample two separate weights

loss steps can be seen (Fig. 8b). The first step (around 7%, w/w) appearing at a temperature of <150 °C corresponds to the loss of water (*i.e.*, adsorbed water on the inner and outer surfaces of SBA-15). The second weight loss (about 475–600 °C) amounts to around 13% (w/w) which is related to the degradation of the polymer. Compared to the PVAm curve, the weight loss of PVAm/SBA-15 is mild, and indicates that PVAm/SBA-15 is more thermo-stable than PVAm. Therefore, after hybridization, the thermal stability is enhanced greatly and this is very important for the catalyst application. For the SA-PVAm/SBA-15 sample, three separate weight losses can be seen (Fig. 8c). The first weight loss (around 4%, w/w) appearing at a temperature of <100 °C, corresponds to loss of water. The second weight loss (around 30%, w/w) at 250–375 °C is related to the degradation of salicylaldehyde which is attached to the surface of the PVAm/SBA-15. The third weight loss of around 6% (w/w) at about 610–680 °C can be related to the degradation of the PVAm chains. However, following coordination to Mn cations, Mn-SA-PVAm/SBA-15 shows higher thermo-stability compared to SA-PVAm/SBA-15. This higher stability indicates that the complex with the metal is formed.

3.2. Catalytic activity

Initially, benzyl alcohol was chosen as a model to test the catalytic activity of the Mn-SA-PVAm/SBA-15 for the oxidation of alcohols under different conditions (Table 2). In order to investigate the effect of solvent, the oxidation of benzyl alcohol (2 mmol) was carried out in several solvents using 0.1 g of the catalyst at 65 °C (Table 2, entries 1–5). As can be seen, normal hexane was not a suitable solvent for this catalytic system, because its polarity was not high enough. The yield of the reaction in water was very low, maybe because water can hydrolysis the C=N bond of the catalyst, and also the mass transfer is probably retarded because water may form a film layer on the catalyst surface, and thus the possibility of diffusing to active sites was reduced.³² Reaction in methanol led to a good yield (80%) and selectivity (90%) during the oxidative reaction, and acetonitrile was the best solvent with

Table 2 Oxidation of benzyl alcohol (2 mmol) with TBHP over Mn-SA-PVAm/SBA-15 under different conditions

Entry	Solvent	T (°C)	Catalyst (g)	TBHP (mmol)	Yield ^a (%)	Selectivity (%)
1	<i>n</i> -hexane	65	0.1	3	70	>99
2	Methanol	65	0.1	3	80	90
3	Water	65	0.1	3	30	80
4	Solvent-free	65	0.1	3	60	90
5	Acetonitrile	65	0.1	3	80	>99
6	Acetonitrile	reflux	0.1	3	90	>99
7	Acetonitrile	25	0.1	3	48	>99
8	Acetonitrile	40	0.1	3	65	>99
9	Acetonitrile	reflux	0.08	3	80	>99
10	Acetonitrile	reflux	0.12	3	90	>99
11	Acetonitrile	reflux	0.14	3	90	>99
12	Acetonitrile	reflux	0.1	2	65	>99
13	Acetonitrile	reflux	0.1	4	75	90
14	Acetonitrile	reflux	0.1	5	65	80
15	Acetonitrile	reflux	—	3	5	>99

^a Isolated yield after 20 min.

80% yield and selectivity of more than 99%, and was chosen as the solvent for further investigation. Reaction in solvent-free conditions gave 60% yield of benzaldehyde.

The effect of temperature was studied in the range 25–81 °C in acetonitrile (Table 2, entries 5–8). The yield increased from 48% to 90% upon increasing the temperature from 25 °C to 81 °C, without any substantial loss of selectivity (>99%).

The effect of the amount of catalyst on the reaction was also investigated. Generally, there was 5% yield in the absence of catalyst (Table 2, entry 15), indicating that this was indeed an Mn-SA-PVAm/SBA-15 catalyzed reaction and the yield was increased by the catalyst. The optimum amount of catalyst (0.1 g) was determined from experiments corresponding to entries 6 and 9–11 in Table 2. No improvement in the yield was found with further increase in the amount of catalyst. Hence, the optimal amount of catalyst was chosen as 0.1 g based on 2.0 mmol of benzyl alcohol. Then, the best amount of the TBHP was determined for the oxidation of benzyl alcohol (Table 2, entries 6 and 12–14). The yield increased from 65 to 90% upon increasing the amount of TBHP from 2 to 3 mmol. Upon further increasing the amount of TBHP, the yield was decreased. This may be due to the blocking of active sites of the catalyst by water molecules from the TBHP solution.³³

The variation of the catalytic activity with the amount of salicylaldehyde, Mn and SBA-15 in the catalyst on the oxidation reaction was investigated. The results are summarized in Table 3. The best yield of benzaldehyde was obtained by using catalyst containing 25 mmol of salicylaldehyde per gram of PVAm/SBA-15 (Table 3, entries 1–6). Higher amounts of salicylaldehyde did not improve the yield to a great extent. On the other hand, it was shown that the yield of the reaction in the presence of Mn-SA-PVAm/SBA-15 as a catalyst was higher than that with Mn-PVAm/SBA-15 (Table 3, entry 1). The higher activity of Mn-SA-PVAm/SBA-15 is due to the existence of the salicylaldehyde Schiff base ligand as an electron donating ligand which facilitates the electron transfer. Also, there was an upward trend of the benzaldehyde yield upon increasing the amount of Mn from 5 to 20 mmol per g of SA-PVAm/SBA-15 (Table 3, entries 6–9). Upon further increasing

the amount of coordinated manganese, the yield remained constant. In order to study the effect of the amount of SBA-15 on the oxidation reaction, several catalysts with various ratios of SBA-15 to PVAm were prepared (Table 3, entries 9–11). The results showed that the yield of benzaldehyde was increased upon increasing the amount of SBA-15 in the catalyst. These results are due to the large surface area of the Mn-SA-PVAm/SBA-15 in comparison with Mn-SA-PVAm. When the amount of SBA-15 is increased, the polymeric material is ordered in the surface of catalyst. So the functional groups of the polymer are free and more effective for salicylaldehyde grafting. The best ratio of SBA-15 to acryl amide was found to be 4 (w/w).

In order to show the generality and scope of the new protocol, several benzylic alcohols were oxidized in the presence of Mn-SA-PVAm/SBA-15 (Scheme 2 and Table 4). In all cases, the oxidation reaction proceeded smoothly to give the corresponding benzaldehyde in moderate to good yields. The reaction with benzylic alcohols carrying electron-donating or electron-withdrawing groups gave the corresponding product in good yields and high purity.

The recycling performance of the Mn-SA-PVAm/SBA-15 in the oxidation reaction was also investigated. After each reaction, the catalyst was filtered, washed with dry methanol (2 × 5 mL), dried at room temperature and reused in the next run without further purification. The catalyst could be reused at least 5 times without appreciable decrease in yield and reaction rate.

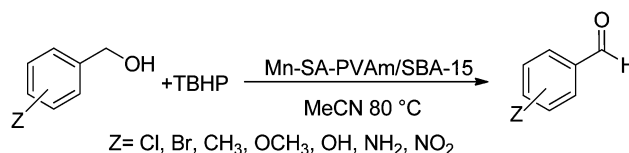
In order to prove the heterogeneous nature of the catalyst and the amount of Mn leaching, a heterogeneity test was performed, in which the catalyst (Mn-SA-PVAm/SBA-15) was separated from the reaction mixture at approximately 50% conversion of the starting material through centrifugation. The reaction progress in the filtrate was monitored (Fig. 9). No further oxidation reaction occurred even at extended times, indicating that the nature of the reaction process was heterogeneous and there was no progress for the reaction in the homogeneous phase.

In addition, to investigate the effect of SBA-15 on the heterogeneity of the catalyst and prevention of Mn leaching, another experiment was performed, in which the catalyst was prepared without SBA-15, with the same amounts of the other materials (Mn-SA-PVAm). Then, the reaction progress was monitored over this catalyst and the amount of Mn leaching was measured in the solution. The same reaction was carried out over the Mn-SA-PVAm/SBA-15 and the amount of Mn leaching was calculated under the same conditions. The results are shown in Table 5. According to the results, Mn-SA-PVAm showed less catalytic activity than Mn-SA-PVAm/SBA-15 which can be related to a greater amount of Mn leaching in the Mn-SA-PVAm system. Therefore, it can be

Table 3 Oxidation of benzyl alcohol over different Mn-SA-PVAm/SBA-15 catalysts^a

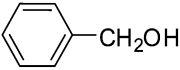
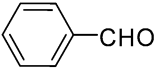
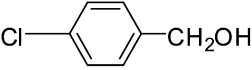
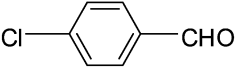
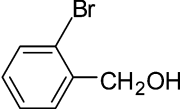
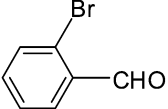
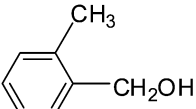
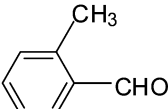
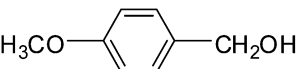
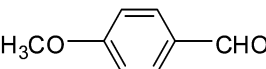
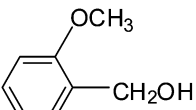
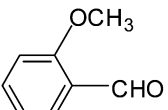
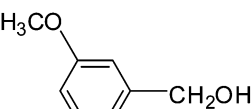
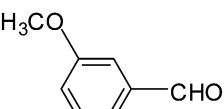
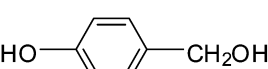
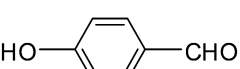
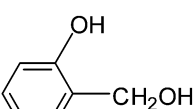
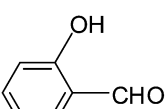
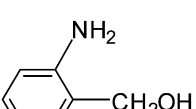
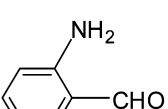
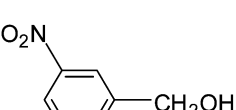
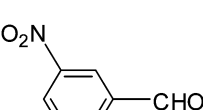
Entry	Salicylaldehyde (mmol per g of PVAm/SBA-15)	Mn (mmol per g of SA-PVAm/SBA-15)	SBA-15 (g per g of AA)	Yield ^b (%)
1	—	10	2	50
2	5	10	2	60
3	10	10	2	65
4	15	10	2	70
5	20	10	2	75
6	25	10	2	80
7	25	5	2	70
8	25	15	2	82
9	25	20	2	85
10	25	20	1	75
11	25	20	4	90

^a Reaction conditions: benzyl alcohol (2 mmol), catalyst (0.1 g), TBHP (3 mmol), acetonitrile (5 mL), reflux, 20 min. ^b Isolated yield with more than 99% selectivity.



Scheme 2 Oxidation of benzylic alcohols catalyzed by Mn-SA-PVAm/SBA-15.

Table 4 Oxidation of benzylic alcohols over Mn-SA-PVAm/SBA-15^a

Entry	Substrate	Product	Time (min)	Yield ^b (%)
1			20	90
2			20	85
3			30	83
4			30	73
5			20	70
6			35	70
7			35	75
8			30	30
9			30	40
10			40	50
11			25	50

^a Reaction conditions: alcohol (2 mmol), TBHP (3 mmol), catalyst (0.1 g), CH₃CN (5 mL), reflux. ^b Isolated yield with more than 99% selectivity.

concluded that the mesoporous structure of SBA-15 prevents Mn leaching and this mesoporous structure acts as a proper cage (micro reactor) for the active species of the catalyst.

According to the above results, we can say that SBA-15 plays two important roles in this composite. One of the greatest advantages of Mn-SA-PVAm/SBA-15 is its ease of use due to its powdery structure. Mn-SA-PVAm is adhesive and this char-

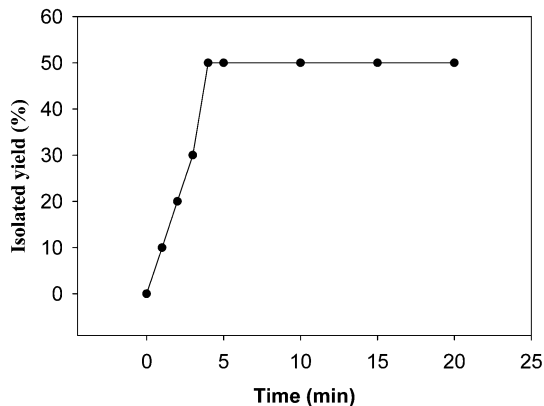


Fig. 9 Heterogeneity test for the oxidation reaction.

Table 5 Effect of SBA-15 on catalytic activity

Catalyst	Yield (%) ^{ab}	Mn leaching (ppm)
Mn-SA-PVAm/SBA-15	90	0.4
Mn-SA-PVAm	50	2.1

^a Reaction conditions: benzyl alcohol (2 mmol), catalyst (0.1 g), TBHP (3 mmol), acetonitrile (5 mL), reflux, 20 min. ^b Isolated yield with more than 99% selectivity.

acter makes it hard to separate it from the vessel, but after mixing with SBA-15 and making the Mn-SA-PVAm/SBA-15 composite, it becomes a powder, which is easy to be used and recycled. Additionally, a comparative reaction using Mn-SA-PVAm/SBA-15 and Mn-SA-PVAm showed that Mn-SA-PVAm/SBA-15 is more efficient, due to completion of the reaction in a short time, which is related to the lower amount of Mn leaching. Actually, in this composite, SBA-15 is a micro reactor for the active species of the catalyst and the reaction occurs in it.

A comparative study was conducted for the use of Mn-SA-PVAm/SBA-15 with some of the reported catalysts for the oxidation of benzyl alcohol with respect to the catalyst, oxidant, reaction time, yield and selectivity of the products (Table 6). It is noteworthy that the oxidation reactions with reported catalysts were carried out with longer reaction times and the benzaldehyde was obtained in low yield, selectivity or

both. The results clearly show that Mn-SA-PVAm/SBA-15 promotes the reaction more effectively than the other catalysts.

4. Conclusion

In summary, we have found that Mn-SA-PVAm/SBA-15 is a new, efficient and environmentally benign catalyst for the oxidation of alcohols in high yield, selectivity and purity. This composite was prepared by a very simple method without using any organosilica precursors (organosilica precursors are expensive and using them involves complicated synthesis and purification methods). Also, heterogenization increased the activity of the homogeneous catalyst due to site-isolation and cooperative effects between the SBA-15 support and the metal complexes. Additionally, the ordered mesostructure of the material also plays an important role in obtaining high reactivity and selectivity towards the oxidation reaction. Therefore, easy preparation without using expensive organosilica precursors, high thermal stability, high catalyst activity, good reusability, and environmental friendliness are some of the catalyst advantages. Further applications of this catalyst to other transformations are currently under investigation.

Acknowledgements

The support by Islamic Azad University, Shahreza Branch (IAUSH) Research Council and Center of Excellence in Chemistry is gratefully acknowledged.

References

- 1 R. A. Sheldon and J. K. Kochi, *Metal-Catalyzed Oxidation of Organic Compounds*, Academic Press, New York, 1981.
- 2 N. E. Leadbeater and M. Marco, *Chem. Rev.*, 2002, **102**, 3217.
- 3 K. C. Gupta and H. K. Abdulkadir, *J. Macromol. Sci., Part A: Pure Appl. Chem.*, 2008, **45**, 53.
- 4 A. A. Costa, G. F. Ghesti, J. L. de Macedo, V. S. Braga, M. M. Santos, J. A. Dias and S. C. L. Dias, *J. Mol. Catal. A: Chem.*, 2008, **282**, 149.
- 5 N. S. Venkataramanan, S. Premsingh, S. Rajagopal and K. Pitchumani, *J. Org. Chem.*, 2003, **68**, 7460.

Table 6 Comparison of Mn-SA-PVAm/SBA-15 with some other catalysts for the oxidation of benzyl alcohol

Entry	Catalyst	Time	Solvent	Oxidant	Yield (%)	Selectivity (%)	Ref.
1	TEMPO, Cu(II) catalyst	2 h	H ₂ O	O ₂	25	86	34
2	CoO-CeO ₂	9 h	<i>n</i> -hexane	TBHP	55	—	35
3	Cr(salen)-NH ₂ -MCM-41	4 h	Solvent free	H ₂ O ₂	52	99	15
4	Alkali-treated ZSM-5	4 h	H ₂ O	H ₂ O ₂	53	86	36
5	Zn ₂ [Fe(CN) ₆]·3H ₂ O	3 h	Solvent free	H ₂ O ₂	28	99	37
6	TiO ₂ -supported nano Au	5 h	Solvent free	O ₂ in ScCO ₂	90	93	38
7	Mg _{2.5} Ni _{0.5} Al HT	6 h	Toluene	O ₂	60	97	39
8	Mn-SA-PVAm/SBA-15	20 min	CH ₃ CN	TBHP	90	>99	This work

- 6 I. F. J. Vankelecom and P. A. Jacobs, Catalyst immobilisation on inorganic supports, in *Chiral Catalyst Immobilisation and Recycling*, ed. P. A. Jacobs, I. F. J. Vankelecom, D. De Vos, Wiley-VCH, Weinheim, Germany, 2000.
- 7 P. Oliveira, A. Machado, A. M. Ramos, I. Fonseca, F. M. Braz Fernandes, A. M. Botelho do Rego and J. Vital, *Microporous Mesoporous Mater.*, 2009, **120**, 432.
- 8 Y. Guo, C. Hu, C. Jiang, Y. Yang, S. Jiang, X. Li and E. Wang, *J. Catal.*, 2003, **217**, 141.
- 9 J. Hu, K. Li, W. Li, F. Ma and Y. Guo, *Appl. Catal., A*, 2009, **364**, 211.
- 10 S. A. Patel, S. Sinha, A. N. Mishra, B. V. Kamath and R. N. Ram, *J. Mol. Catal. A: Chem.*, 2003, **192**, 53.
- 11 E. D. P. Carreiro and A. J. Burke, *J. Mol. Catal. A: Chem.*, 2006, **249**, 123.
- 12 G. Grivani, S. Tangestaninejad and A. Halili, *Inorg. Chem. Commun.*, 2007, **10**, 914.
- 13 J. Zhao, J. Han and Y. Zhang, *J. Mol. Catal. A: Chem.*, 2005, **231**, 129.
- 14 B. Z. Zhan and A. Thomposon, *Tetrahedron*, 2004, **60**, 2917.
- 15 X. Wang, G. Wu, J. Li, N. Zhao, W. Wei and Y. Sun, *J. Mol. Catal. A: Chem.*, 2007, **276**, 86.
- 16 M. Zanetti, S. Lomakin and G. Camino, *Macromol. Mater. Eng.*, 2000, **279**, 1.
- 17 C. Yang, P. H. Liu, Y. F. Ho, C. Y. Chiu and K. J. Chao, *Chem. Mater.*, 2003, **15**, 275.
- 18 M. T. Run, S. Z. Wu, D. Y. Zhang and G. Wu, *Mater. Chem. Phys.*, 2007, **105**, 341.
- 19 G. Kickelbick, *Prog. Polym. Sci.*, 2003, **28**, 83.
- 20 S. S. Ray and O. Masami, *Prog. Polym. Sci.*, 2003, **28**, 1539.
- 21 D. A. Ruddy, N. L. Ohler, A. T. Bell and T. D. Tilley, *J. Catal.*, 2006, **238**, 277.
- 22 L. Jiao and J. R. Regalbuto, *J. Catal.*, 2008, **260**, 342.
- 23 A. H. Lu and F. Schuth, *Adv. Mater.*, 2006, **18**, 1793.
- 24 Y. Jung, S. Kim, S. J. Park and J. M. Kim, *Colloids Surf., A*, 2008, **313**, 292.
- 25 C. Hess, U. Wild and R. Schlögl, *Microporous Mesoporous Mater.*, 2006, **95**, 339.
- 26 R. J. Kalbasi, M. Kolahdoozan and M. Rezaei, *Mater. Chem. Phys.*, 2011, **125**, 784.
- 27 R. J. Kalbasi, M. Kolahdoozan, A. R. Massah and K. Shahabian, *Bull. Korean Chem. Soc.*, 2010, **31**, 2618.
- 28 R. J. Kalbasi, M. Kolahdoozan, K. Shahabian and F. Zamani, *Catal. Commun.*, 2010, **11**, 1109.
- 29 M. Colilla, F. Balas, M. Manzano and M. V. Regi, *Chem. Mater.*, 2007, **19**, 3099.
- 30 D. Y. Zhao, J. L. Feng, Q. S. Huo, N. Melosh, G. H. Fredrickson, B. F. Chmelka and G. D. Stucky, *Science*, 1998, **279**, 548.
- 31 M. Salavati-Niasari, S. N. Mirsattari and M. Bazarganipour, *Polyhedron*, 2008, **27**, 3653.
- 32 Y. Chujo and T. Saegusa, *Adv. Polym. Sci.*, 1992, **100**, 11.
- 33 K. M. Parida and D. Rath, *Appl. Catal., A*, 2007, **321**, 101.
- 34 P. J. Figiel, A. M. Kirillov, Y. Y. Karabach, M. N. Kopylovich and A. J. L. Pombeiro, *J. Mol. Catal. A: Chem.*, 2009, **305**, 178.
- 35 S. S. Deshpande and R. V. Jayaram, *Catal. Commun.*, 2008, **9**, 186.
- 36 A. Jia, L. L. Lou, C. Zhang, Y. Zhang and S. Liu, *J. Mol. Catal. A: Chem.*, 2009, **306**, 123.
- 37 S. R. Ali, V. K. Bansal, A. A. Khan, S. K. Jain and M. A. Ansari, *J. Mol. Catal. A: Chem.*, 2009, **303**, 60.
- 38 X. Wang, H. Kawanami, S. E. Dapurkar, N. S. Venkataramanan, M. Chatterjee, T. Yokoyama and Y. Ikushima, *Appl. Catal., A*, 2008, **349**, 86.
- 39 T. Kawabata, Y. Shinozuka, Y. Ohishi, T. Shishido, K. Takaki and K. Takehira, *J. Mol. Catal. A: Chem.*, 2005, **236**, 206.